Research Square

Preprints are preliminary reports that have not undergone peer review.
They should not be considered conclusive, used to inform clinical practice,
or referenced by the media as validated information.

Effects of NRF-1 and PGC-1α Cooperation on HIF-1α and Rat Cardiomyocyte Apoptosis Under Hypoxia

Nan Niu
School of Basic Medicine, Ningxia Medical University https://orcid.org/0000-0002-5123-6625
Hui Li
School of Basic Medicine, Ningxia Medical University
Xiancai Du
School of Basic Medicine, Ningxia Medical University
Chan Wang
School of Basic Medicine, Ningxia Medical University
Junliang Li
School of Basic Medicine, Ningxia Medical University
Jihui Yang
School of Basic Medicine, Ningxia Medical University
Cheng Liu
School of Basic Medicine, Ningxia Medical University
Songhao Yang
School of Basic Medicine, Ningxia Medical University
Yazhou Zhu
School of Basic Medicine, Ningxia Medical University
Wei Zhao (zw-6915@163.com)
School of Basic Medicine, Ningxia Medical University

Research Article

Keywords: NRF-1, apoptosis, cardiomyocytes, hypoxia, HIF-1α

Posted Date: December 13th, 2021

DOI: https://doi.org/10.21203/rs.3.rs-181724/v2

License: This work is licensed under a Creative Commons Attribution 4.0 International License. Read Full License

Abstract

Hypoxia is a primary inducer of cardiomyocyte injury, its significant marker being hypoxia-induced cardiomyocyte apoptosis. Nuclear respiratory factor-1 (NRF-1) and hypoxia-inducible factor (HIF)-1α are transcriptional regulatory elements implicated in multiple biological functions, including oxidative stress response. However, their roles in hypoxia-induced cardiomyocyte apoptosis remain unknown. The effect HIF-α, together with NRF-1, exerts on cardiomyocyte apoptosis also remains unclear. We established a myocardial hypoxia model and investigated the effects of these proteins on the proliferation and apoptosis of rat cardiomyocytes (H9C2) under hypoxia. Further, we examined the association between NRF-1 and HIF-1α to improve the current understanding of NRF-1 anti-apoptotic mechanisms. The results showed that NRF-1 and HIF-1α are important anti-apoptotic molecules in H9C2 cells under hypoxia, although their regulatory mechanisms differ. NRF-1 could bind to the promoter region of *Hif-1α* and negatively regulate its expression. Additionally, HIF-1β exhibited competitive binding with NRF-1 and HIF-1α, demonstrating a synergism between NRF-1 and the peroxisome proliferator-activated receptor-gamma coactivator-1α. These results indicate that cardiomyocytes can regulate different molecular patterns to tolerate hypoxia, providing a novel methodological framework for studying cardiomyocyte apoptosis under hypoxia.

Introduction

Hypoxia is characterized by insufficient blood supply resulting from various factors. It is the primary cause of cardiomyocyte injury [1,2]. Apoptosis is one of the primary forms of myocardial cell death [3,4], and hypoxia-induced apoptosis is a strong indicator of myocardial damage. We previously found that nuclear respiratory factor-1 (NRF-1) alleviates myocardial cell damage caused by cobalt chloride, an anoxic chemical agent, by inhibiting apoptosis [5]. NRF-1, a 68 kDa nuclear transcription regulator initially detected during a study on cytochrome c activation and expression [6], plays an important role in integrating the interaction between the nucleus and mitochondria, inducing mitochondrial gene expression and regulating energy metabolism [7,9]. Subsequent studies on NRF-1 structure and function and mitochondrial oxidative respiration, which is closely associated with cell growth, immune response, apoptosis, embryonic development, and stress-response regulation in the endoplasmic reticulum [10–13]. However, reports on NRF-1 effects on cardiomyocyte apoptosis under hypoxia are limited. Contradictory functions of NRF-1, with one study demonstrating that its overexpression increased cell sensitivity to apoptosis [11], while another suggesting that it may activate mitochondrial biogenesis-related genes to achieve an anti-apoptotic effect [14], have been reported. Moreover, NRF-1 requires coactivators, such as peroxisome proliferator-activated receptor gamma coactivator 1-alpha (PGC-1α), for regulating its target genes. NRF-1 transcription can be enhanced by binding to PGC-1α [15], a transcription factor capable of synergizing with other transcription factors to regulate gene expression as well as other cellular physiological and metabolic reactions, such as mitochondrial biogenesis, apoptosis, and cell-fate determination [16,17]. Therefore, the regulatory effect of NRF-1 on cardiomyocyte apoptosis may depend on PGC-1α co-participation.

Hypoxic reactions are primarily characterized by a series of subsequent molecular events caused by reduced or completely depleted oxygen content. Hypoxia-inducible factors (HIFs) are a class of nuclear transcription regulatory factors closely related to physiological responses to hypoxia. They are divided into three subtypes, with α and β subunits each: HIF-1α and β, HIF-2α and β, and HIF-3α and β. HIF levels increase steadily under hypoxia, and these proteins contribute to the cellular oxygen stress response [18,20]. HIF-1 is, presently, one of the most widely studied molecules. Under normoxic conditions, proline residues on HIF-1α are hydroxylated by prolyl hydroxylase, which is recognized and ubiquitinated by E3 ubiquitin ligase, and rapidly degraded by proteasomes. However, under hypoxia, proline hydroxylase (uses oxygen as auxiliary matrices) is inhibited, leading to HIF-1α accumulation in the cytoplasm, followed by its entry into the nucleus where it combines with HIF-1β to form a dimer that regulates the expression of downstream genes [21]. Whole-genome chromatin immunoprecipitation (ChIP) analysis revealed that the promoter region of several genes possesses a HIF-1-binding element (5'-A/TCGTG-3, Hypoxia Response Element, HRE). This element can trigger various metabolic reactions, including those related to cell energy metabolism, vascular regeneration, cell proliferation, and immune and inflammatory reactions [22–24]. HIF-1α also suppresses rat brain cell apoptosis during cerebral ischemia–reperfusion injury, by influencing B-cell lymphoma (BCL)-2 expression and participating in the regulation of p53 and phosphatidylinositol 3 kinase/protein kinase B apoptotic pathway [25–28]. However, the mechanistic role of HIF-1 in hypoxia-induced cardiomyocyte apoptosis remains unclear. Additionally, the NRF-1–HIF-1 relationship under hypoxia, and NRF-1 effect on cardiomyocyte apoptosis remain uncharacterized.

Since hypoxia-induced cardiomyocyte apoptosis is a major risk factor for cardiac failure, preventing cardiomyocyte apoptosis under hypoxia is of particular importance. NRF-1 can alleviate cardiomyocyte apoptosis and enhance cell viability; however, the underlying mechanism remains elusive. Although several important associations between the HIF-1 dimer and hypoxia stress and apoptosis have been documented, a gap of knowledge regarding cardiomyocyte apoptosis under hypoxia persists. Additionally, the NRF-1–HIF-1 relationship under hypoxia, and NRF-1 effect on cardiomyocyte apoptosis remain uncharacterized. Whether a regulatory interaction between NRF-1 and HIF-1α exists and potentially affects cardiomyocyte apoptosis warrants further research. This study aimed to examine the effect of NRF-1 on cardiomyocyte apoptosis by establishing a hypoxia model of cardiomyocytes, to study the interaction between NRF-1 and HIF-1α independently and in relation to apoptosis under hypoxia. Our objective is to provide new therapeutic alternatives and a theoretical basis for the treatment and intervention of heart failure.

Materials And Methods

2.1. Cell culture

H9C2 and 293T cells were purchased from the Chinese Academy of Sciences (Shanghai, China); 293T cells were used to package lentivirus and H9C2 cells were employed to construct cell lines and in related experimental studies. The plasmids used in this study were used to transform *Escherichia coli*, followed by amplification, clonal selection, enzyme digestion, sequencing, and further amplification to obtain the required plasmids.

2.2. Construction of lentivirus-transfected cardiomyocytes

All transfection reagents were obtained from PolyJet^{TM} (Signagen Company, Jinan City, China). Further, 293T cells were subcultured in a 10-cm culture dish; at 80%–90% confluency, the original medium was discarded and 5 mL fresh Dulbecco's modified Eagle's medium (DMEM, Gibco, NY, USA) supplemented with 10% fetal bovine serum (FBS, Gibco) was added. Cells were incubated for 30–60 min. For each 10-cm cell culture dish, plasmid suspension was prepared in 500 μL serum-free DMEM in a 1:1 ratio of packaging plasmid to lentiviral expression plasmid (pLP1:pLP2:pLPVSVG:pCDH-CMV/pGreenPuro/sh-NRF1/sh-HIF1α at a ratio of 1:1:1:1, 6 μg each) and subjected to vortex oscillation. Then, 500 μL serum-free DMEM was mixed with 60 μL PolyJet^{TM} transfection reagent, mixed gently, and added to the plasmid mixture and allowed to stand for 15 min at 20 °C. After 48 h, the virus particles were collected by centrifugation at 4 °C, 50,000 ´ *g* for 2 h (ultrahigh-speed). Next, 1 × 10^6 H9C2 cells were seeded on a six-well plate. Once cells adhered, the supernatant was discarded, and 2 mL lentiviral transfection suspension containing 2% FBS and 8 μg/μL polybrene (Sigma-Aldrich, Germany) was added. After 72 h, the fluorescence intensity was measured. The cells were screened after treatment with 1 mg/mL puromycin (Sigma-Aldrich) for 2 weeks. After another week of culture, the stably transfected cells were screened using an ARIA III flow cytometer (BD Company, NJ, USA). The empty vector cardiomyocytes were named pCDH-CMV and pGreenPuro; the NRF-1-overexpressing, NRF-1-inhibited, and HIF-1α-inhibited cardiomyocytes were named pCDH-NRF1, sh-NRF1, and sh-HIF1α, respectively.

2.3. Establishment of the hypoxia model

The cells were subcultured in three T-75 cell culture bottles, and the experiment was initiated when the cells reached 90% confluence. A day before hypoxia induction, 1 × 10^7 cells were subcultured in a 10-cm culture dish and placed in an incubator at 37 ℃ overnight for subsequent use. On day 2 under anoxia, the medium was removed and 10 mL cell culture medium was added to each dish. The dishes were placed in a three-gas incubator, and the timer was set to start when the oxygen concentration reached 1%. After completion, the nitrogen valve in the anoxic operation table was opened, and the oxygen concentration detection table was used to reduce the oxygen concentration to 1%. After treatment under hypoxia, the cells were rapidly placed in the anoxic operation table to extract total protein or RNA.

2.4. Western blotting

The primary components of the pyrolysis solution were: 50 mM Tris-HCl (Sigma-Aldrich), 150 mM NaCl (Sigma-Aldrich), 1% Triton X-100 (Sigma-Aldrich), 1% sodium deoxycholate (Sigma-Aldrich), 0.1% SDS (Sigma-Aldrich), and 5 mM EDTA (Sigma-Aldrich). To this, 200 μg/μL aprotinin (Sigma-Aldrich), 1 μg/μL leupeptin (Sigma-Aldrich), 1 mM PMSF (Solarbio Life Science, Beijing, China), 10 mM $MgCl_2$ (Thermo Fisher Scientific, Waltham, MA, USA), and 40 U benzonase nuclease (Haigen Biotech, Sanghai, China) were added. All processes were performed on ice. To each 10-cm culture dish, 1 mL of the prepared lysate was added. The cells were scraped and added to a microcentrifuge tube and maintained for 15 min, shaken for 10 s every 5 min, and centrifuged at 12,000 ´ *g* for 15 min. The supernatant was collected and 100 μL was mixed with 25 μL protein loading buffer, boiled at 100 °C for 10 min, and subjected to western blotting. After total protein extraction, 20 μL protein was loaded. The conditions for electrophoresis were: 120 V for 15 min and 150 V for 55 min. After electrophoresis, the proteins were transferred to a polyvinylidene fluoride (PVDF, Sigma-Aldrich) membrane under a constant current (300 mA) for 2 h. The PVDF membrane was placed in a buffer solution containing PBS (Solarbio Life Science) and 0.05% Tween 20 (Solarbio Life Science) and sealed for 4 h. The antibody dilutions used were: DNA methyltransferase (DNMT)-1 (24206-1-AP, 1:1,000; Protech, Rosemont, IL, USA), HIF-1α (NB100-105, 1:1,000; Novus Biologicals, Briarwood, CO, USA), HIF-1β (NB100-124, 1:1,000; Novus Biologicals), PGC-1α (NBP1-04676, 1:1,000; Novus Biologicals), NRF-1 (ab175932, 1:2,000; Abcam, Cambridge, UK), β-actin (ab49900, 1:10,000, HRP-conjugated; Abcam), BCL-2 (sc-7382, 1:500; Santa Cruz Biotechnology Inc., TX, USA), BCL-2-associated X protein (Bax; ab32503, 1:2,000; Abcam), and BCL-extra-large (BCL-xL; ab32370, 1:1,000; Abcam). The membranes were treated with the primary antibody overnight at 4 °C, followed goat anti-rabbit (Bioss Antibodies, Beijing, China) and goat anti-mouse (Bioss Antibodies) secondary antibodies (1:25,000) for 4 h. After washing the membrane with PBST, the protein levels were measured using a ChemiDoc MP Imaging System (Bio-Rad Laboratories, Hercules, CA, USA). Image Lab 5.1 (Bio-Rad Laboratories) was used to analyze gray values.

2.5. Immunoprecipitation

Lysate preparation and total protein extraction were performed as described in 2.4. For western blotting, 100 μL supernatant was used, and the remaining was used for immunoprecipitation. The samples were stored on ice until further use. Each 900 μL protein lysate sample was mixed with 1 μg immunoprecipitation antibodies and placed in the microcentrifuge tube rack of a rotary mixer. The instrument was placed in a refrigerator at 4 °C overnight. The next day, 1 μL pre-mixed magnetic beads (Thermo Fisher Scientific) was added to the sample, mixed gently, and incubated in a refrigerator at 4 °C for 1 h. The liquid was then discarded, and 900 μL pre-cooled lysis buffer containing a protease inhibitor was added, gently mixed and washed thrice. Next, 50 μL 1× protein loading buffer (Solarbio Life Science) was added, mixed well, boiled at 100 °C for 10 min, incubated on ice, and stored. The subsequent steps were the same as described in 2.4.

2.6. ChIP assay

The cells were spread on 10-cm Petri dishes with a convergence degree of approximately 90%. To every culture dish, 10 mL DMEM and 275 μL fresh 37% formaldehyde (Sigma-Aldrich) were added, and cross-linking was allowed for 10 min. Next, 10× glycine was added to quench excess formaldehyde, and the suspension was mixed and incubated for 5 min. The residual medium was discarded, 10 mL pre-cooled PBS was added, and the cells were washed. Then, 1

mL pre-cooled PBS containing a protease inhibitor was added. The cells were then scraped into a microcentrifuge tube and centrifuged at 700 ´ *g* at 4 °C for 3 min. The supernatant was discarded, and the cells were resuspended in SDS lysis buffer containing a protease inhibitor and incubated on ice before ultrasonication (Xinzhi Biotechnology Co., Ltd, Ningbo, China). The ultrasonication conditions were: power, 50 W; ultrasonication for 5 s, stop for 55 s, repeated eight times. Next, protein-G agarose beads (Thermo Fisher, Norway) were added to the ultrasonicated products and mixed for 1 h on the rotary mixer at 4 °C. The supernatant was collected by centrifugation and distributed into two microcentrifuge tubes. Next, 1 μg of normal rat IgG (Sangon Biotech, Shanghai, China) and 1 μg antibody were added to the two tubes, and the mixture was incubated overnight at 4 °C. The next day, agarose beads were added to trap the protein–DNA complexes, followed by washing, complex elution using an eluent buffer, and DNA purification after cross-linking. Primer sequences for Hif-1α promoter region used in this study are listed in Table 1.

Table 1. Primer sequences for *Hif-1α* promoter region

Bases upstream of *Hif-1α* promoter	Primer sequence (5′–3′)	Size (bp)
-1922 to -1511	F: ATCGCCCTATGTGGTTTC R: AAGGTCCTGGCTTCAAAA	412
-1331 to -1135	F: CATTATTATACAACCCAACG R: CAAGCCCAACAAAGGAAC	197
-1147 to -1020	F: TTTGTTGGGCTTGGAATA R: TGTGCTGGGAACTATGGA	128
-997 to -815	F: GTCTGTAGGTTGGAGGATG R: GAGTGACAAGGCAGGAAA	183
-641 to -455	F: TAATGACTTGGAGACTTCCCTT R: TCCTTAGTTGCGTGGTTG	187
-472 to -200	F: CAACCACGCAACTAAGGA R: AATCAGGAGGAGGTCAGC	273
-199 to -19	F: AGAGCAACGTGGGCTGGGGTGG R: AGGGGAGGGGAGCAAAGG	146
-447 to -113	F: CCAACCACGCAACTAAGGA R: AGAGCCAATGGGAAAGGAC	334
-447 — +136	F: CCAACCACGCAACTAAGGA R: TTGCTCCTCCGGCTGGCTTGTC	583
-191 to +136	F: GCTGACCTCCTCCTGATTG R: TTGCTCCTCCGGCTGGCTTG	327
-191 to +374	F: GCTGACCTCCTCCTGATTGG R: CGGCCCGGCTTACTTT	565

2.7. Polymerase chain reaction (PCR)

DNA extracted using a DNA extraction kit (Omega Biotek, Inc., Norcross, GA, USA) or purified DNA from the ChIP assay was used as the template. The primer sequences are listed in Supplementary Table S1. The reaction system and related reagents are listed in Supplementary Table S2. The reaction conditions were as follows: pre-denaturation at 95 °C for 2 min; 30 cycles of denaturation at 95 °C for 15 s, annealing at 55–65 °C for 15 s, extension at 68 °C for 10 s; and preservation at 4 °C. The samples were separated by electrophoresis using a 0.5% agarose gel.

2.8. RNA extraction

RNA was extracted using TRIzol reagent (Thermo Fisher Scientific). Briefly, 2–5 × 10^6 cells were subcultured in six-well plates. TRIzol reagent (1 mL) was added to each well, and the suspension was distributed in enzyme-free microcentrifuge tubes. Next, 200 μL chloroform (Sigma-Aldrich) was added; the mixture was shaken for 15 s, incubated on ice for 15 min, and centrifuged at 12,000 ´ *g* for 15 min. To the collected supernatant, an equal volume of isopropanol was added, mixed well, incubated on ice for 10 min, and centrifuged at 12,000 ´ *g* for 10 min. The supernatant was discarded; 75% ethanol was added to the pellet and the solution was centrifuged at 7,500 ´ *g* for 5 min. After air-drying, 50 μL enzyme-free ddH_2O was added to dissolve RNA, and the samples were stored at −80 °C for subsequent experiments.

2.9. Reverse transcription

A cDNA Reverse Transcription Kit (Thermo Fisher Scientific) was used for the reverse transcription. The reaction system is outlined in Supplementary Table S3.

2.10 Real-time qPCR

The qPCR reagent was purchased from DBI Bioscience (Ludwigshafen, Germany). After preparing the reaction system, a real-time PCR amplification instrument (StepOne™ Real-Time PCR System, Thermo Fisher Scientific) was used for performing PCR. The reaction conditions were: pre-denaturation at 95 °C for 2 min; denaturation at 95 °C for 15 s, annealing at 60 °C for 30 s, cycling at 72 °C for 30 s; generation of dissolution curve, cycling at 95 °C for 15 s, annealing at 60 °C for 30 s, and cycling at 72 °C for 30 s. The template quality and primer specificity were determined from the dissolution and amplification curves. The target gene mRNA levels were calculated using the $2^{-\triangle\triangle CT}$ method; rat β-actin was used as an internal reference control. The reaction system and primer sequences are listed in Supplementary Table S4 and Supplementary Table S5, respectively.

2.11. Real-time evaluation of cell proliferation

Before evaluating cell proliferation, the cells were counted and the concentration was adjusted to 15×10^5 cells/mL/well. Real-time cell analysis (ACEA Biosciences, CA, USA) was used. The detection time was adjusted to measure the cell proliferation level every 10 min for 24–48 h. The cells in each well were labeled, and 150 µL complete medium was added into the special plate (8-well) to deduct the base value. Next, 300 µL cell suspension was added into each well, and the cell state was assessed microscopically (EVOS™ XL Core Imaging System, Thermo Fisher). After evenly spreading out the suspension, the plates were placed on an ultra-clean workbench for 30 min and then transferred to the instrument, with the entire detector placed in the cell incubator. After adherence overnight, the cells were observed. For hypoxic cultures, after overnight adherence, the entire instrument was placed in the three-gas incubator, and cells were observed after the oxygen concentration was adjusted to 1%.

2.12. Evaluation of caspase-3 activity

Cells ($5–10 \times 10^6$ cells) were seeded on a 10-cm cell culture dish 1 day in advance. The next day, 10 µL DTT was added per mL of lysis buffer and detection buffer. After hypoxic or normoxic culturing, the medium was discarded, and 500 µL of the aforementioned cold cell lysate was added. The cells were scraped into a microcentrifuge tube, mixed by vibration at high speed for 15 s, placed on ice for 15 min with shaking for 15 s every 5 min, and centrifuged at 12,000 ´ *g* for 15 min. The supernatant was collected into a fresh tube, and protein levels were quantified using the Bradford assay. A 96-well plate was prepared for each group, and three repeat wells were assigned. Next, 10 µL protein supernatant (containing 30–50 µg of total protein) was collected from each well, the lysate was added, and the suspension was mixed well. Thereafter, 10 µL Ac-DEVD-pNA (BestBio, Nanjing, China) was added, and the culture was incubated in the dark at 37 °C for 4 h until the solution turned yellow. Detection was performed by measuring absorbance at 405 nm. Caspase-3 activity was measured based on the ratio of the treated group absorbance to that of the blank control group.

2.13. Real-time observation of cell apoptosis

The experiment was performed in a Cytation 5 Imaging Reader (BioTek, VT, USA). Briefly, the plate bottom height was adjusted, the six-well plate mode was selected, and 1×10^6 cells were seeded in the six-well plate. After overnight adherence at 37 °C, the plate was placed on a test bench. The focus, exposure time, channel, and other parameters were adjusted, and red and blue fluorescence were detected simultaneously for each well, once every 10 min. The temperature was set at 37 °C, and the oxygen concentration was fixed at 1%. Automatic imaging and videography were performed. The cell proliferation curve was generated using the Gen5 software (BioTek).

2.14. Bisulfite sequencing PCR

DNA was extracted according to the method described in 2.7. Based on the sequence predicted by the MethPrimer tool [29–31], primers were designed for DNA extraction. Details of the reaction system and primer sequences are outlined in Supplementary Tables S6 and S7, respectively. The reaction conditions were: Pre-denaturation at 95 °C for 5 min; 35 cycles of denaturation at 95 °C for 30 s, annealing at 55–60 °C for 30 s, and extension at 72 °C for 45 s; and extension for 10 min at 72 °C. The sequencing process was commissioned to Sangon Biotech.

The gene sequence is as follows (5'–3'):

GAGAGCAA**CG**TGGGCTGGGGTGGGGCCTGGC**CG**CCTG**CG**TCCTTTCCCATTGGCTCT**CG**GGGAACC**CG**CCTC**CG**CTCAGGTGAGG**CG**GGCC**CGCG**GGTG**CGCGCG**T**C**

After bisulfite treatment, the cytosine residues were changed to thymine, with the CG sites retained as “C,” as shown in the following sequence (5'–3'):

GAGAGTAA**CG**TGGGTTGGGGTGGGGTTTGGT**CG**TTTG**CG**TTTTTTTTTATTGGTTTT**CG**GGGAATT**CG**TTTT**CG**TTTAGGTGAGG**CG**GGTT**CGCG**GGTG**CGCGCG**T**C**

2.15. Statistical analysis

SPSS 17.0 (IBM Corporation, NY, USA) was used for statistical analysis. The results are expressed as mean ± standard deviation. Student's *t*-test was used to compare the means of two samples. One-way analysis of variance was used for comparing multiple samples. Student–Newman–Keuls test was used for pairwise comparison between groups. $P < 0.05$ was considered statistically significant.

Results

3.1. NRF-1 affects cardiomyocyte apoptosis

For a preliminary investigation of the effect of NRF-1 on cardiomyocyte apoptosis under hypoxia, we used H9C2 cells at 1% oxygen concentration. First, we developed an NRF-1-overexpressing cardiomyocyte cell line (pCDH-NRF1) and an NRF-1-inhibited cardiomyocyte cell line (sh-NRF1; Table S1) and studied their proliferation. Under normoxia (21% O_2, 5% CO_2, 74% N_2), NRF-1 promoted cell proliferation; however, its inhibition decreased cardiomyocyte proliferation decreased. Under hypoxia (1% O_2, 5% CO_2, 94% N_2), cardiomyocyte proliferation was restricted in all groups; subsequently, NRF-1 overexpression significantly alleviated the decline in cell proliferation, while its inhibition aggravated the hypoxia-induced suppression of cell proliferation (Fig. 1A, B). These results indicate the protective effects of NRF-1 in hypoxia-induced cardiomyocyte injury.

To further verify whether the protective effect of NRF-1 is mediated by its anti-apoptotic effect, the different levels of cardiomyocyte apoptosis were evaluated. Caspase-3 is crucial for the execution of apoptosis. Activated caspase-3 can cleave DNA or induce its degradation to RNA, inhibit cytoskeletal protein synthesis, and ultimately induce nuclear pyknosis, fragmentation, and cell membrane disintegration [32,33]. Under hypoxia, caspase-3 activity increased gradually, and NRF-1 suppressed this increase (Fig. 2A). Furthermore, with the prolongation in hypoxia duration and caspase 3 activation, the state of myocardial cells in each group gradually deteriorated, and the cells began to disintegrate and undergo pyknosis and nuclear fragmentation. As cell membrane integrity is lost during cell apoptosis, propidium iodide can enter the damaged nucleus and stain the DNA. Apoptotic and necrotic cells showed bright red fluorescence, with peak fluorescence at approximately 6 h; however, NRF-1 delayed this process to approximately 10 h (Fig. S1). Next, we compared the expression of the apoptosis regulatory molecules and found that with an increase in hypoxia, the expression of NRF-1 and anti-apoptotic proteins BCL-2 and BCL-xL decreased, whereas that of pro-apoptotic protein Bax marginally increased, suggesting that NRF-1 promoted BCL-2/BCL-xL expression and inhibited Bax expression (Fig. 2B, C). These results suggest that in hypoxia-induced myocardiocyte injury, NRF-1 offers protection from apoptosis.

3.2. NRF-1 binds to *Hif-1α* promoter region and inhibit its expression

In 293T cells, NRF-1 reportedly binds to *Hif-1α* promoter region and negatively regulates its expression [34]. The regulatory effects of NRF-1 on HIF-1α were therefore investigated. The primers were designed from the sequence of the rat *Hif-1α* promoter region available on the Ensembl genome browser (https://asia.ensembl.org/index.html). After evaluating each primer annealing temperature, ChIP was performed to confirm the NRF-1 binding site in *Hif-1α* promoter region. Our data showed that the promoter region between -1992–-1511 and -1147–-455 upstream of *Hif-1α* represented the NRF-1 binding site (Fig. 3A). To better elucidate the effect of NRF-1 on the binding site, qPCR was performed. We observed that *HIF-1α* expression decreased significantly with the increase in NRF-1 expression (Fig. 3B). Similar results were obtained in the western blotting experiment, wherein the HIF-1α protein levels increased gradually with the prolongation of the duration of hypoxia; however, its expression could be inhibited by NRF-1 (Fig. 3C). The above data suggest that the binding of NRF-1 to *Hif-1α* promoter region can inhibit its expression.

Additionally, NRF-1 reportedly activates *Dnmt-1* promoter region, influence its expression, regulate methylation levels, and further influence the expression of other genes [34,35]. Since NRF-1 can inhibit the HIF-1α expression at the transcriptional level, we investigated whether this regulation involves its methylation. First, the PROMO online analysis tool (http://alggen.lsi.upc.es/cgi-bin/promo_v3/promo/promoinit.cgi?dirDB=TF_8.3) was used to predict NRF-1 binding sites in *Dnmt1* promoter region. Since PROMO does not have a rat genome resource, the human database was referred for the binding sequence and it was compared with the rat *Dnmt1* promoter sequence to identify the corresponding sequence. The data showed that NRF-1 has two binding sites in the promoter region of human *DNMT1*, and comparison with rat *Dnmt1* promoter sequence revealed two similar sequences, suggesting that the binding sequence is conserved. Subsequently, primers for the sequence were designed (Fig. S2 A, B). After optimizing the annealing temperature, the ChIP assay was performed and revealed that NRF-1 could bind to the sequence (Fig. S2C). Next, the effect of NRF-1 overexpression on the DNMT-1 protein level was evaluated using western blotting. The results indicate that under hypoxia (for 0, 1, 2, 3, 6, 12, and 24 h), *Dnmt1* expression gradually decreased; however, it significantly increased following NRF-1 overexpression (Fig. S2D). Hence, we next determined whether NRF-1 modulates HIF-1α expression by regulating its methylation through DNMT-1, leading to subsequent regulation of *Hif-1α* transcription. Based on the information provided on the MethPrimer website (https://www.urogene.org/methprimer/), we concluded that a CpG island was present in *Hif-1α* promoter region. The methylation status of *Hif-1α* promoter before and after hypoxia was compared. The bisulfite sequencing PCR results revealed no significant change in the methylation status of the predicted sequences (Fig. S2E, F). Thus, NRF-1-mediated regulation of DNMT-1 expression does not affect HIF-1α; NRF-1 directly inhibits HIF-1α.

3.3. HIF-1α inhibition by NRF-1 affects cardiomyocyte apoptosis

To evaluate the effect of HIF-1α inhibition by NRF-1 on cardiomyocyte apoptosis, HIF-1α and NRF-1 were simultaneously inhibited under artificial conditions. Preliminary experiments showed that hypoxia for 1 and 2 h did not induce a marked oxygen stress response. Accordingly, hypoxia duration was set at 0, 3, 6, 12, and 24 h. Our data showed that HIF-1α suppression exacerbated the hypoxia-induced decline in cell proliferation and promoted caspase-3 activity; however, contrary to our expectation, NRF-1 expression increased along with BCL-2 and BCL-xL protein levels. These results indicate that similar to NIF-1, HIF-1α acts as an anti-apoptotic protein; furthermore, a mutually inhibitory relationship might exist between NRF-1 and HIF-1α, and the increased BCL-2 and BCL-xL levels could result from the increase in NRF-1 expression caused by HIF-1α inhibition. To further evaluate these possibilities, HIF-1α and NRF-1 expression was inhibited. Compared with HIF-1α inhibition (sh-HIF1α) under hypoxia, the dual inhibition of NRF-1 and HIF-1α relieved the decline in cell proliferation and lowered caspase-3 activity. Unexpectedly, with the reduction in NRF-1 expression, the levels of BCL-2 and BCL-xL decreased, whereas the levels of HIF-1α

increased (Fig. 4A, B, C). These results indicate that although NRF-1 primarily regulates the expression of BCL-2 and BCL-xL, this is not the only mechanism that modulates apoptosis. Therefore, HIF-1α may regulate apoptosis under hypoxia in a BCL-2/BCL-xL-independent manner.

3.4. NRF-1 competes with HIF-1α to bind HIF-1β

Previous results suggested that HIF-1α might exert the same anti-apoptotic effect as NRF-1. Concurrently, the results also showed that NRF-1 and HIF-1α exhibited mutual expression inhibition. Next, we analyzed the effect exerted by this mutual inhibition. HIF-1α forms a dimer with HIF-1β, and this complex has several biological functions. This led us to investigate NRF-1 and HIF-1β interaction and its effect on other molecular events. Moreover, the effect of this interaction on HIF-1α and HIF-1β binding warranted investigation. First, the binding among HIF-1α, NRF-1, and HIF-1β following NRF-1 interference (sh-NRF1) was evaluated. The results showed that similar to HIF-1α, NRF-1 could bind to HIF-1β, and the level of this binding gradually decreased with the prolongation of hypoxia. Compared with the empty vector group (pGreenPuro), the NRF-1 inhibition group (sh-NRF1) showed a decrease in NRF-1–HIF-1β binding, and HIF-1α–HIF-1β binding increased simultaneously (Fig. 5A). These results indicated that a competitive binding interaction might exist between NRF-1 and HIF-1α for HIF-1β under hypoxia.

We evaluated the effect of NRF-1 inhibition on HIF-1α–HIF-1β binding. To effectively confirm the binding effect, cells were treated with dimethyloxallyl glycine (DMOG) and BAY 87-2243 (HY-15836, BAY 87-2243, MedChemExpress, NJ, USA). DMOG stabilizes HIF-1α expression and enhances its cytoplasmic accumulation by inhibiting HIF prolyl hydroxylase [36,37]. BAY 87-2243 is a highly effective selective inhibitor of HIF-1α expression. Neither of the two drugs affects HIF-1β expression. Immunoblotting showed that DMOG enhances HIF-1α expression in a dose-dependent manner; with increase in DMOG concentration, NRF-1 expression gradually decreased without affecting HIF-1β expression. Additionally, immunoprecipitation revealed that DMOG increased HIF-1α–HIF-1β binding but decreased NRF-1–HIF-1β binding. Next, we suppressed HIF-1α expression to study the interaction between NRF-1 and HIF-1α under hypoxia. The results showed that BAY 87-2243 effectively inhibited the hypoxia-induced increase in HIF-1α expression, and consistent with the previous finding, NRF-1 expression increased with HIF-1α inhibition; following BAY 87-2243-mediated HIF-1α inhibition, NRF-1–HIF-1β binding increased (Fig. 5B, C). These findings further confirmed the competitive binding between NRF-1 and HIF-1α.

3.5. PGC-1α participates in the competitive binding of NRF-1 and HIF-1α with HIF-1β

The regulatory effect of NRF-1 on cells is inseparable from the synergistic effect of PGC-1α. The role of PGC-1α was thus investigated. PGC-1α expression decreased gradually with an increase in hypoxia duration, whereas NRF-1 inhibition did not alter PGC-1α expression. Immunoprecipitation confirmed a stable binding relationship between PGC-1α and NRF-1 that did not change with hypoxia duration. Then, the effect of this binding relationship on HIF-1α was evaluated. DMOG inhibited PGC-1α, and PGC-1α could bind to HIF-1β; however, PGC-1α binding reduced, similar to NRF-1, with an increase in DMOG concentration and HIF-1α accumulation. Subsequently, the cells were treated with ZLN005 (HY-17538; MedChemExpress, NY, USA), a drug that activates PGC-1α transcription and expression. This demonstrated that for different durations of hypoxia (0, 6, 12, and 24 h), PGC-1α intervention increased NRF-1 expression and decreased HIF-1α expression, without affecting HIF-1β expression. However, the increase in PGC-1α expression induced by ZLN005 enhanced the binding between NRF-1 and HIF-1β and suppressed the binding between HIF-1α and HIF-1β (Fig. 6A, B, C). These results indicate a novel binding mechanism among NRF-1/PGC-1α, HIF-1α, and HIF-1β.

Discussion

Apoptosis accompanies ischemia- and hypoxia-induced myocardiocyte injury [38]. Cardiomyocyte apoptosis is common to almost all types of heart diseases [38–42]. To alleviate the effect or avoid the occurrence of cardiomyocyte apoptosis, especially the extensive damage it causes under hypoxia injury, extensive studies were conducted. NRF-1 overexpression alleviated cardiomyocyte apoptosis induced by chemical hypoxia. To further investigate effects of NRF-1 on cardiomyocyte apoptosis, especially under actual hypoxic conditions, we used three-gas incubators to reduce the oxygen concentration to 1%. We found that NRF-1 overexpression and inhibition affected cell growth and proliferation under normoxic conditions. While NRF-1 overexpression promoted cell growth, its inhibition suppressed cell proliferation. Thus, NRF-1 can promote cell proliferation, and NRF-1 inhibition affects cell division and growth, consistent with the finding that NRF-1 knockout is lethal in mouse embryos [43]. This established the important role of NRF-1 in the cell viability and growth of individual organisms. Subsequently, we studied the effect of NRF-1 on cardiomyocyte proliferation under different durations of hypoxia. In the first few hours (6 h) under hypoxia, the cells maintained a certain proliferation level that may be attributed to the residual oxygen in the solution. However, progressive depletion of oxygen with increase in hypoxia duration decreased the cardiomyocyte proliferation in each group. Notably, NRF-1 overexpression significantly slowed the decline in cell proliferation, whereas its inhibition significantly decreased the cell proliferation. This indicates that NRF-1 can protect cardiomyocytes from hypoxia and highlights the anti-apoptotic mechanism adopted by NRF-1.

The decrease in cell proliferation under hypoxia may be caused by cell necrosis, apoptosis, and autophagy. To further identify the role of apoptosis in hypoxia, we observed the levels of apoptosis-related molecules, including caspase-3—the primary executor of apoptosis. In transgenic mice, caspase-3 overexpression increased the infarct size of cardiomyocytes caused by oxygen stress and increased the likelihood of death [44]. Conversely, caspase-3 downregulation reduced the apoptotic index and improved cardiac function after myocardial infarction [45,46]. We first assessed caspase-3 activity in different groups of cardiomyocytes under hypoxia to determine whether the decrease in cardiomyocyte proliferation was caused by apoptosis. Caspase-3 activity gradually increased with increase in the duration of hypoxia. Additionally, NRF-1 overexpression alleviated the high caspase-3 activity; after NRF-1 inhibition, caspase-3 activation became more pronounced. Subsequently, real-time dynamic observation of cell growth showed that the nuclear red fluorescence became more evident with increase in caspase-3 activity. As the severity of nuclear membrane damage increased, nuclear condensation increased as well. However, NRF-1 overexpression significantly inhibited this process. These results further indicate that hypoxia-induced damage caused to cardiomyocytes is partly triggered by apoptosis; since NRF-1 can alleviate apoptosis, it can prevent the damage caused to cardiomyocytes under hypoxia.

Previous studies on NRF-1 have primarily focused on its effect on mitochondrial function; NRF-1 regulates the expression of mitochondrial respiratory chain complex gene family members, affecting mitochondrial biogenesis, and increases mitochondrial ATP production [47,48]. Reportedly, NRF-1 significantly improves the mitochondrial membrane potential in cardiomyocytes under hypoxia and enhances the mitochondrial respiratory capacity to increase cardiomyocyte viability [5]. Therefore, the anti-apoptotic effect of NRF-1 may be achieved by regulating apoptosis-related proteins associated with the mitochondria. Most of these molecules belong to the BCL-2 family, including pro-apoptotic molecules, such as Bax, Bak, and Bid, and anti-apoptotic molecules, such as BCL-2 and BCL-xL. At high levels, Bax can form dimers with other pro-apoptotic molecules, such as Bak and Bad, thus forming pore channels in the mitochondrial membrane, resulting in cytochrome c release and altered mitochondrial membrane potential, eventually triggering apoptosis. BCL-2 and BCL-xL competitively bind to Bax to reverse the effects of Bax binding to other apoptotic triggers, thus achieving an anti-apoptotic effect. The interaction between anti-apoptotic and pro-apoptotic BCL-2 family proteins can directly determine the fate of different cardiac pathological processes, including myocardial infarction, dilated cardiomyopathy, and ischemic heart disease [49]. For example, BCL-2 can significantly reduce the infarct size caused by apoptosis [16,50], while BCL-xL can inhibit the expression of the pro-apoptotic molecules Bax and Bid through different mechanisms [51]. Our results showed that decreased NRF-1 expression caused the expression of the anti-apoptotic molecules BCL-2 and BCL-xL to decrease, while that of the pro-apoptotic molecule Bax was not affected. Since NRF-1 expression can be upregulated via human intervention, this increase can induce subsequent upregulation of BCL-2 and BCL-xL expression, thereby preventing or delaying their hypoxia-induced downregulation. Although Bax level did not increase significantly with hypoxia, NRF-1 could inhibit its expression. Thus, the anti-apoptotic effect of NRF-1 on cardiomyocytes under hypoxia is achieved by promoting the expression of BCL-2/BCL-xL and inhibiting Bax expression.

Our results indicate that NRF-1 exerts an anti-apoptotic effect in hypoxia-induced cardiomyocyte injury. The specific mechanism or the molecular control method adopted by NRF-1 for regulating the process remains to be studied. The central element in hypoxia is the reduction in oxygen concentration. Studying the specific genes related to oxidative stress and the regulation of cardiomyocyte apoptosis by proteins encoded by these genes may help understand the regulatory mechanism. HIF family proteins are extremely sensitive to oxygen; they are degraded by proteases under normoxia, but remain stable under hypoxia. HIF-1 affects apoptosis under hypoxia and in cardiac diseases in various ways [52,53]. Therefore, we first assessed whether NRF-1 targets HIF-1α. Transcription factors generally modulate molecular regulation by controlling the transcription levels of genes. Consistently, NRF-1 inhibited *Hif-1α* mRNA expression and led us to determine whether the effect is directly inhibited by binding or mediated by other regulatory processes. Although NRF-1 exhibits a competitive relationship with methylation, it could promote DNMT-1 expression [35] to maintain the methylation level and further regulate spermatogenesis [13]. In addition to maintaining methylation levels, DNMT-1 initiates methylation [52,54]. Since NRF-1 inhibits the expression of HIF-1α, we investigated the effect of increased methylation levels caused by methyltransferase-1 on the above relationship and found that NRF-1 could bind to *Dnmt1* promoter region and regulate its expression, consistent with previous reports [13]. Subsequent studies showed that DNMT-1 expression decreases under prolonged hypoxia, whereas NRF-1 overexpression delayed this decline. Notably, according to an existing prediction website (http://alggen.lsi.upc.es/cgi-bin/promo_v3/promo/promoinit.cgi?dirDB=TF_8.3) and the contributions of previous reports [13], an NRF-1-binding sequence is found in human and mouse *Dnmt1*. Furthermore, we found a corresponding sequence in rats, suggesting the conservation of this binding sequence and highlighting the important regulatory role of NRF-1 in DNMT-1 expression. However, even though *Hif-1α* promoter region predictably possessed a methylation site, there was no significant change in the methylation status before and after hypoxia, as shown by bisulfite sequencing PCR. Possibly, methylation is not the primary regulatory event affecting HIF-1α expression. Based on these results, we conclude that NRF-1 negatively regulates HIF-1α expression by directly binding to *Hif-1α* promoter region.

Previous studies have shown that HIF-1α acts as a protective molecule in cardiomyocytes under stress [55,56]. It enhances cardiac tolerance to hypoxia in various ways, for instance, by enhancing anaerobic respiration and nucleotide metabolism and reducing cellular oxidative stress [57–60]. However, HIF-1α can also induce apoptosis, increase the myocardial infarct area, and promote damage [61,62]. Therefore, the effect of HIF-1α on the heart remains to be completely deciphered. We confirmed the effect of HIF-1α on apoptosis of rat cardiomyocytes under hypoxia through experimental studies. HIF-1α inhibition reduced cardiomyocyte proliferation under normoxia; however, following hypoxia, the proliferation of cardiomyocytes in the HIF-1α inhibition group decreased more significantly, and caspase-3 activity increased. These results indicate that HIF-1α exerts a protective effect on cardiomyocytes under hypoxia. To elucidate the negative regulatory effect of NRF-1 on HIF-1α and the effect of NRF-1 on cardiomyocyte apoptosis, we specifically inhibited NRF-1 expression in coordination with HIF-1α inhibition. Under normoxia, the inhibition of both molecules reduced cardiomyocyte proliferation; however, compared with that in the HIF-1α inhibition group, the reduction in cardiomyocyte proliferation level was alleviated in the NRF-1 inhibition group, and caspase-3 activity was suppressed. Further analysis showed that HIF-1α inhibition increased BCL-2 and BCL-xL expression, and BCL-2/BCL-xL levels were relatively lower in the NRF-1 and HIF-1α co-inhibition group than that in the HIF-1α inhibition group. Interestingly, HIF-1α inhibition led to an increase in NRF-1 expression, which has not been previously reported. This novel finding could also explain the simultaneous increase in BCL-2/BCL-xL expression with HIF-1α and NRF-1 inhibition. Superficially, HIF-1α inhibition leads to cardiomyocyte injury and apoptosis under hypoxia, indicating that HIF-1α serves as an anti-apoptotic molecule under hypoxia. However, under the simultaneous inhibition of NRF-1, the cell morphology appeared qualitatively better than that in the HIF-1α inhibition group; this may be related to the fact that NRF-1 inhibition can partially restore HIF-1α levels and alleviate, to a certain extent, cardiomyocyte hypoxia-induced injury. The results are concordant with the protective effect of HIF-1α on cardiomyocytes previously reported and suggest that HIF-1α plays a more significant anti-apoptotic role than NRF-1. The specific inhibition of HIF-1α expression was accompanied by an increase in BCL-2/BCL-xL expression, whereas after the simultaneous inhibition of NRF-1, BCL-2/BCL-xL expression decreased with a relative increase in HIF-1α expression; these findings were consistent with those reported by Choi et al. [63], Menrad et al. [64], and Zhao et al. [62], and indicated that BCL-2/BCL-xL is primarily affected by NRF-1 rather than HIF-1α. These results suggest that apoptosis caused by NRF-1-mediated inhibition of HIF-1α may not involve BCL-2 family proteins but occurs via hitherto unknown mechanisms.

Since NRF-1 and HIF-1α exert the same anti-apoptotic effect, it is worth investigating why they exhibit mutual inhibition. Whether the mutual inhibition is associated with the similar anti-apoptotic effects and the antagonism between the two molecules remains unclear. HIF-1α regulates downstream genes by forming a dimer with HIF-1β. The involvement of NRF-1 in this dimer formation remains to be determined. However, our results demonstrated that NRF-1 could also bind to HIF-1β, and the binding levels gradually decreased under prolonged hypoxia, which reciprocally affected the binding with HIF-1α. Additionally, the

inhibition of NRF-1 expression led to an increase in HIF-1α and HIF-1β binding, suggesting a possibility of competitive binding between HIF-1α and HIF-1β. We used DMOG and BAY 87-2243 to verify our hypothesis and found that these drugs did not affect HIF-1β expression while regulating HIF-1α expression. DMOG promoted HIF-1α expression, inhibited NRF-1 expression, and suppressed the binding between NRF-1 and HIF-1β. However, when BAY 87-2243 was used to inhibit HIF-1α, a contrasting yet consistent phenomenon was observed—HIF-1α inhibition increased NRF-1 expression, as well as the binding levels of NRF-1 and HIF-1β. This phenomenon may be related to the adaptation of cells to hypoxic stress. Thus, under normal conditions, NRF-1 acts as a key transcription factor that exerts multiple effects on cardiomyocyte molecular regulation. In the absence of external stimulation, NRF-1 and other nuclear molecules, including HIF-1β, form a key complex and participate in the regulation of mitochondrial function, cell growth, and metabolism. However, under prolonged hypoxia, the expression of NRF-1 decreases gradually, leading to the loss of cell function. As an adaptation to hypoxia and to promote survival, HIF-1α accumulates, gradually replacing NRF-1, thereby promoting the binding between HIF-1α and HIF-1β. Certain key molecules, such as CD39, CD73, p53, and LDHA, are expressed, facilitating cell tolerance to hypoxia. This could explain why HIF-1α can promote hypoxia tolerance in cardiomyocytes and aggravate cardiomyocyte injury under different hypoxic conditions [65,66]. However, the exact reason for aggravation of cardiomyocyte injury needs to be investigated.

Lastly, we examined the role of PGC-1α that is reportedly involved in processes related to apoptosis regulation, such as p53 gene-mediated apoptosis, enhancement of mitochondrial recovery to reduce apoptosis, and regulation of the expression of apoptosis-related molecules [67–69]. We found that PGC-1α levels gradually decreased with the increase of hypoxia duration, and this change was not affected by NRF-1 inhibition, indicating that PGC-1α is a transcription factor operating upstream of NRF-1. This finding was consistent with previous reports [70,71]. Our results also showed that NRF-1 and PGC-1α formed stable dimers, and the binding levels of NRF-1 and PGC-1α did not change as the duration of hypoxia was prolonged. Upon DMOG stimulation, the same effect observed for NRF-1 was observed. Promoting PGC-1α expression with ZLN005 treatment, resulted in increased levels of NRF-1 as well, and the levels of NRF-1 and HIF-1β binding increased during the initial stages of hypoxia (0 and 6 h), whereas the binding between HIF-1α and HIF-1β was suppressed. However, the enhanced binding effect was gradually reversed by HIF-1α because the levels of the two molecules decreased with the increase in the duration of hypoxia. These results suggest that PGC-1α, as an upstream transcription regulator of NRF-1, is also involved in regulating the competitive binding between NRF-1 and HIF-1α. However, whether PGC-1α directly binds to HIF-1α or indirectly binds to HIF-1β by binding with NRF-1 needs to be studied further.

Conclusion

Our results indicate that NRF-1 can alleviate cardiomyocyte apoptosis and improve cardiomyocyte viability under hypoxia. Moreover, HIF-1α serves as an important anti-apoptotic molecule under hypoxia. To the best of our knowledge, this is the first study to report that NRF-1 cooperatively acts with PGC-1α and competes with HIF-1α to bind HIF-1β. This molecular regulatory process may be related to cardiomyocyte adaptation to hypoxia and may promote cell survival under low-oxygen stress. This study provides a novel theoretical framework for improving the protective mechanisms for hypoxia-induced myocardial injury; however, the specific molecular process warrants further investigation.

Declarations

Acknowledgments

The authors thank the members of the Institute of Medical Sciences of Ningxia Hui Autonomous Region for providing excellent technical assistance.

Declaration of Competing interests

The authors declare no competing interests.

Funding

This work was supported by the Natural Science Foundation of Ningxia Hui Autonomous Region [grant number 2020AAC03425].

Authors' contributions

Nan Niu and Wei Zhao designed and revised the experiment. Nan Niu wrote the manuscript. Nan Niu, Hui Li, Xiancai Du and Junliang Li performed main experiment, Jihui Yang and Cheng Liu performed the cell sorting. Chan Wang, Songhao Yang performed the packaging of the virus. Chan Wang and Yazhou Zhu performed the cell images.

References

1 Y. Rustamova, M. Lombardi, Ischemic Heart Disease. Cardiac Magnetic Resonance Atlas, first ed., Springer International Publishing, 2020.

2 J.J. Savla, B.D. Levine, H.A. Sadek, The effect of hypoxia on cardiovascular disease: friend or foe?, High Alt. Med. Biol. 19 (2018) 124–130. https://doi.org/10.1089/ham.2018.0044.

3 G.M. Virzì, A. Clementi, C. Ronco, Cellular apoptosis in the cardiorenal axis, Heart Fail. Rev. 21 (2016)177–189. https://doi.org/10.1007/s10741-016-9534-y.

4 Y. Xuan, S. Liu, Y. Li, J. Dong, J. Luo, T. Liu, Y. Jin, Z. Sun, Short-term vagus nerve stimulation reduces myocardial apoptosis by downregulating microRNA205 in rats with chronic heart failure, Mol. Med. Rep. 16 (2017) 5847–5854. https://doi.org/10.3892/mmr.2017.7344.

5 N. Niu, Z. Li, M. Zhu, H. Sun, J. Yang, S. Xu, W. Zhao, R. Song, Effects of nuclear respiratory factor-1 on apoptosis and mitochondrial dysfunction induced by cobalt chloride in H9C2 cells, Mol. Med. Rep. 19 (2019) 2153–2163. https://doi.org/10.3892/mmr.2019.9839.

6 L. Gopalakrishnan, R.C. Scarpulla, Structure, expression, and chromosomal assignment of the human gene encoding nuclear respiratory factor 1, J. Biol. Chem. 270 (1995) 18019–18025. https://doi.org/10.1074/jbc.270.30.18019.

7 C.M. Chau, M.J. Evans, R.C. Scarpulla, Nuclear respiratory factor 1 activation sites in genes encoding the gamma-subunit of ATP synthase, eukaryotic initiation factor 2 alpha, and tyrosine aminotransferase. Specific interaction of purified NRF-1 with multiple target genes, J. Biol. Chem. 267 (1992) 6999–7006.

8 W. Gao, M. Wu, N. Wang, Y. Zhang, Y. Wang, Increased expression of mitochondrial transcription factor A and nuclear respiratory factor-1 predicts a poor clinical outcome of breast cancer, Oncol. Lett. 15 (2018) 1449–1458. https://doi.org/10.3892/ol.2017.7487.

9 H.B. Suliman, T.E. Sweeney, C.M. Withers, C.A. Piantadosi, Co-regulation of nuclear respiratory factor-1 by NFkappaB and CREB links LPS-induced inflammation to mitochondrial biogenesis, J. Cell Sci. 123 (2010) 2565–2575. https://doi.org/10.1242/jcs.064089.

10 A.H. Remels, N.A. Pansters, H.R. Gosker, A.M. Schols, R.C. Langen, Activation of alternative NF-κB signaling during recovery of disuse-induced loss of muscle oxidative phenotype, Am. J. Physiol. Endocrinol. Metab. 306 (2014) E615–E626. https://doi.org/10.1152/ajpendo.00452.2013.

11 F. Morrish, C. Giedt, D. Hockenbery, c-MYC apoptotic function is mediated by NRF-1 target genes, Genes Dev. 17 (2003) 240–255. https://doi.org/10.1101/gad.1032503.

12 B.N. Radde, M.M. Ivanova, H.X. Mai, N. Alizadeh-Rad, K. Piell, P. Van Hoose, M.P. Cole, P. Muluhngwi, T.S. Kalbfleisch, E.C. Rouchka, B.G. Hill, C.M. Klinge, Nuclear respiratory factor-1 and bioenergetics in tamoxifen-resistant breast cancer cells, Exp. Cell Res. 347 (2016) 222–231. https://doi.org/10.1016/j.yexcr.2016.08.006.

13 J. Wang, C. Tang, Q. Wang, J. Su, T. Ni, W. Yang, Y. Wang, W. Chen, X. Liu, S. Wang, J. Zhang, H. Song, J. Zhu, Y. Wang, NRF1 coordinates with DNA methylation to regulate spermatogenesis, FASEB J. 31 (2017) 4959–4970. https://doi.org/10.1096/fj.201700093R.

14 C.A. Piantadosi, M.S. Carraway, A. Babiker, H.B. Suliman, Heme oxygenase-1 regulates cardiac mitochondrial biogenesis via Nrf2-mediated transcriptional control of nuclear respiratory factor-1, Circ. Res. 103 (2008) 1232–1240. https://doi.org/10.1161/01.RES.0000338597.71702.ad.

15 L. Dangsheng, PGC-1alpha: looking behind the sweet treat for porphyria, Cell 122 (2005) 487–489. https://doi.org/10.1016/j.cell.2005.08.010.

16 S.D. Chen, D.I. Yang, T.K. Lin, F.Z. Shaw, C.W. Liou, Y.C. Chuang, Roles of oxidative stress, apoptosis, PGC-1α and mitochondrial biogenesis in cerebral ischemia, Int. J. Mol. Sci. 12 (2011) 7199–7215. https://doi.org/10.3390/ijms12107199.

17 C.F. Cheng, H.C. Ku, H. Lin, PGC-1α as a pivotal factor in lipid and metabolic regulation, Int. J. Mol. Sci. 19 (2018) 3447. https://doi.org/10.3390/ijms19113447.

18 D. Kung-Chun Chiu, A. Pui-Wah Tse, C.T. Law, I. Ming-Jing Xu, D. Lee, M. Chen, R. Kit-Ho Lai, V. Wai-Hin Yuen, J. Wing-Sum Cheu, D. Wai-Hung Ho, C.M. Wong, H. Zhang, I. Oi-Lin Ng, C. Chak-Lui Wong, Hypoxia regulates the mitochondrial activity of hepatocellular carcinoma cells through HIF/HEY1/PINK1 pathway, Cell Death Dis. 10 (2019) 934. https://doi.org/10.1038/s41419-019-2155-3.

19 H.S. Li, Y.N. Zhou, L. Li, S.F. Li, D. Long, X.L. Chen, J.B. Zhang, L. Feng, Y.P. Li, HIF-1α protects against oxidative stress by directly targeting mitochondria, Redox Biol. 25 (2019) 101109. https://doi.org/10.1016/j.redox.2019.101109.

20 R. Varghese, S. Sridharan, A. Datta, J. Venkatraj, Modeling hypoxia stress response pathways. In IEEE International Workshop on Genomic Signal Processing & Statistics, Houston, TX, USA, 2013. DOI: 10.1109/GENSIPS.2013.6735939

21 G.L. Semenza, Hypoxia-inducible factors in physiology and medicine, Cell 148 (2012) 399–408. https://doi.org/10.1016/j.cell.2012.01.021.

22 T. Jain, E.A. Nikolopoulou, Q, Xu, A. Qu. Hypoxia inducible factor as a therapeutic target for atherosclerosis, Pharmacol. Ther. 183 (2018) 22–33. https://doi.org/10.1016/j.pharmthera.2017.09.003.

23 S. Ke-Yuan, H. Gao-Zhong, Y. Fang, C. Shi-Hong, F. Guo-Xiang, Value of hypoxia-inducible factor 1α in diagnosis and prognosis of acute decompensated chronic heart failure, Journal of Shanghai Jiaotong University (Medical Science). 38 (2018) 426.

24 X. Meng, B. Grötsch, Y. Luo, K.X. Knaup, M.S. Wiesener, X.X. Chen, J. Jantsch, S. Fillatreau, G. Schett, A. Bozec, Hypoxia-inducible factor-1α is a critical transcription factor for IL-10-producing B cells in autoimmune disease, Nat. Commun. 9 (2018) 251. https://doi.org/10.1038/s41467-017-02683-x.

25 Y. Gao, H. Yin, Y. Zhang, Y. Dong, F. Yang, X. Wu, H. Liu, Dexmedetomidine protects hippocampal neurons against hypoxia/reoxygenation-induced apoptosis through activation HIF-1α/p53 signaling, Life Sci. 232 (2019) 116611. https://doi.org/10.1016/j.lfs.2019.116611.

26 Y. Guo, Role of HIF-1a in regulating autophagic cell survival during cerebral ischemia reperfusion in rats, Oncotarget 8 (2017) 98482–98494. https://doi.org/10.18632/oncotarget.21445.

27 D. Trisciuoglio, C. Gabellini, M. Desideri, E. Ziparo, G. Zupi, D. Del Bufalo, Bcl-2 regulates HIF-1a protein stabilization in hypoxic melanoma cells via the molecular chaperone HSP90, PLoS One 5 (2010) e11772. https://doi.org/10.1371/journal.pone.0011772.

28 J. Wei, J. Wu, W. Xu, H. Nie, R. Zhou, R. Wang, Y. Liu, G. Tang, J. Wu, Salvanic acid B inhibits glycolysis in oral squamous cell carcinoma via targeting PI3K/AKT/HIF-1α signaling pathway, Cell Death Dis. 9 (2018) 599. https://doi.org/10.1038/s41419-018-0623-9.

29 L.C. Li, Chromatin remodeling by the small RNA machinery in mammalian cells, Epigenetics 9 (2014) 45–52. https://doi.org/10.4161/epi.26830.

30 V. Portoy, S.H.S. Lin, K.H. Li, A. Burlingame, Z.H. Hu, H. Li, L.C. Li, saRNA-guided Ago2 targets the RITA complex to promoters to stimulate transcription, Cell Res. 26 (2016) 320–35. https://doi.org/10.1038/cr.2016.22.

31 J. Wang, R.F. Place, V. Portnoy, V. Huang, M.R. Kang, M. Kosaka, M.K.C. Ho, L.C. Li, Inducing gene expression by targeting promoter sequences using small activating RNAs, J. Biol. Methods. 2 (2011) e14. https://doi.org/10.14440/jbm.2015.39.

32 B. Khalilzadeh, N. Shadjou, G.S. Kanberoglu, H. Afsharan, M. de la Guardia, H.N. Charoudeh, A. Ostadrahimi, M.R. Rashidi, Advances in nanomaterial based optical biosensing and bioimaging of apoptosis via caspase-3 activity: a review, Mikrochim. Acta. 185 (2018) 434. https://doi.org/10.1007/s00604-018-2980-6.

33 R. Kim, M. Emi, K. Tanabe, Caspase-dependent and -independent cell death pathways after DNA damage (Review), Oncol. Rep. 14 (2005) 595–599.

34 D. Wang, J. Zhang, Y. Lu, Q. Luo, L. Zhu, Nuclear respiratory factor-1 (NRF-1) regulated hypoxia-inducible factor-1α (HIF-1α) under hypoxia in HEK293T, IUBMB Life. 68 (2016) 748–755. https://doi.org/10.1002/iub.1537

35 S. Domcke, A.F. Bardet, P.A. Ginno, D. Hartl, L. Burger, D. Schübeler, Competition between DNA methylation and transcription factors determines binding of NRF1, Nature 528 (2015) 575–579. https://doi.org/10.1038/nature16462.

36 E. Baader, G. Tschank, K.H. Baringhaus, H. Burghard, V. Günzler, Inhibition of prolyl 4-hydroxylase by oxalyl amino acid derivatives in vitro, in isolated microsomes and in embryonic chicken tissues, Biochem. J. 300 (1994) 525–530. https://doi.org/10.1042/bj3000525.

37 K. Schultz, V. Murthy, J.B. Tatro, D. Beasley, Prolyl hydroxylase 2 deficiency limits proliferation of vascular smooth muscle cells by hypoxia-inducible factor-1α-dependent mechanisms, Am. J. Physiol. Lung Cell. Mol. Physiol. 296 (2009) L921– L927. https://doi.org/10.1152/ajplung.90393.2008.

38 P. Xia, Y. Liu, Z. Cheng, Signaling pathways in cardiac myocyte apoptosis, Biomed. Res. Int. 2016 (2016) 9583268. https://doi.org/10.1155/2016/9583268.

39 C. Gill, R. Mestril, A. Samali, Losing heart: the role of apoptosis in heart disease—a novel therapeutic target?, FASEB J. 16 (2002) 135–146. https://doi.org/10.1096/fj.01-0629com.

40 J. Narula, F.D. Kolodgie, R. Virmani, Apoptosis and cardiomyopathy, Curr. Opin. Cardiol. 15 (2000) 183–188. https://doi.org/10.1097/00001573-200005000-00011.

41 O.S. Polunina, L.P. Voronina, G.N. Mukhambetova, G.Y. Maslyaeva, P.N. Voronina, Analysis of level of apoptosis markers in patients with coronary heart disease, Medical Alphabet 4 (2020) 5–8. https://doi.org/10.33667/2078-5631-2019-4-35(410)-5-8.

42 E. Teringova, P.A. Tousek, Apoptosis in ischemic heart disease, J. Transl. Med. 15 (2017) 87. https://doi.org/10.1186/s12967-017-1191-y.

43 L. Huo, R.C. Scarpulla, Mitochondrial DNA instability and peri-implantation lethality associated with targeted disruption of nuclear respiratory factor 1 in mice, Mol. Cell. Biol. 21 (2001) 6449–6454. https://doi.org/10.1128/MCB.21.2.644-654.2001.

44 G. Condorelli, R. Roncarati, J. Ross Jr, A. Pisani, G. Stassi, M. Todaro, S. Trocha, A. Drusco, Y. Gu, M.A. Russo, G. Frati, S.P. Jones, D.J. Lefer, C. Napoli, C.M. Croce, Heart-targeted overexpression of caspase3 in mice increases infarct size and depresses cardiac function, Proc. Natl. Acad. Sci. U. S. A. 98 (2001) 9977–9982. https://doi.org/10.1073/pnas.161120198.

45 H. Liu, S. Liu, X. Tian, Q. Wang, J. Rao, Y. Wang, F. Xiang, H. Zheng, L. Xu, Z. Dong, Bexarotene attenuates focal cerebral ischemia-reperfusion injury via the suppression of JNK/Caspase-3 signaling pathway, Neurochem. Res. 44 (2019) 2809–2820. https://doi.org/10.1007/s11064-019-02902-5.

46 Q. Liu, Lentivirus mediated interference of Caspase-3 expression ameliorates the heart function on rats with acute myocardial infarction, Eur. Rev. Med. Pharmacol. Sci. 18 (2014) 1852–1858.

47 P.F. Hsieh, S.F. Liu, T.J. Hung, C.Y. Hung, G.Z. Liu, L.Y. Chuang, M.F. Chen, J.L.Wang, M.D. Shi, C.H. Hsu, Y.L. Shiue, Y.L. Yang, Elucidation of the therapeutic role of mitochondrial biogenesis transducers NRF-1 in the regulation of renal fibrosis, Exp. Cell Res. 349 (2016) 23–31. https://doi.org/10.1016/j.yexcr.2016.09.005.

48 G. Napolitano, D. Barone, S. Di Meo, P. Venditti, Adrenaline induces mitochondrial biogenesis in rat liver, J. Bioenerg. Biomembr. 50 (2018) 11–19. https://doi.org/10.1007/s10863-017-9736-6.

49 A.B. Gustafsson, R.A. Gottlieb, Bcl-2 family members and apoptosis, taken to heart, Am. J. Physiol. Cell. Physiol. 292 (2007) C45–C51. https://doi.org/10.1152/ajpcell.00229.2006.

50 V. Brocheriou, A.A. Hagège, A. Oubenaïssa, M. Lambert, V.O. Mallet, M. Duriez, M. Wassef, A. Kahn, P. Menasché, H. Gilgenkrantz, Cardiac functional improvement by a human Bcl-2 transgene in a mouse model of ischemia/reperfusion injury, J. Gene Med. 2 (2000) 326–333. https://doi.org/10.1002/1521-2254(200009/10)2:5<326::AID-JGM133>3.0.CO;2-1.

51 A. Garcia, F. Murad, Bcl-xL inhibits tBid and Bax via distinct mechanisms, Faraday Discuss, in press. 2020. doi: 10.1039/D0FD00045K

52 Y. Li, Z. Zhang, J. Chen, W. Liu, W. Lai, B. Liu, X. Li, L. Liu, S. Xu, Q. Dong, et al., Stella safeguards the oocyte methylome by preventing de novo methylation mediated by DNMT1. Nature 564 (2018) 136–140. https://doi.org/10.1038/s41586-018-0751-5.

53 J. Yin, B. Ni, W.G. Liao, Y.Q. Gao, Hypoxia-induced apoptosis of mouse spermatocytes is mediated by HIF-1α through a death receptor pathway and a mitochondrial pathway, J. Cell. Physiol. 233 (2018) 1146–1155. https://doi.org/10.1002/jcp.25974.

54 Svedružić ŽM. Dnmt1 structure and function, Prog. Mol. Biol. Transl. Sci. 101 (2011) 221–254. https://doi.org/10.1016/B978-0-12-387685-0.00006-8.

55 A.L. de Castro, R.O. Fernandes, V.D. Ortiz, C. Campos, J.H.P. Bonetto, T.R.G. Fernandes, A. Conzatti, R. Siqueira, A.V. Tavares, A. Belló-Klein, A.S.D.R. Araujo, Cardioprotective doses of thyroid hormones improve NO bioavailability in erythrocytes and increase HIF-1α expression in the heart of infarcted rats, Arch. Physiol. Biochem. in press. 2020. https://doi.org/10.1080/13813455.2020.1779752.

56 G. Nanayakkara, A. Alasmari, S. Mouli, H. Eldoumani, J. Quindry, G. McGinnis, X. Fu, A. Berlin, B. Peters, J. Zhong, R. Amin, Cardioprotective HIF-1α-frataxin signaling against ischemia-reperfusion injury, Am. J. Physiol. Heart Circ. Physiol. 309 (2015) H867–H879. https://doi.org/10.1152/ajpheart.00875.2014.

57 F. Lin, L.H. Pan, L. Ruan, W. Qian, R. Liang, W.Y. Ge, B. Huang, Differential expression of HIF-1α, AQP-1, and VEGF under acute hypoxic conditions in the non-ventilated lung of a one-lung ventilation rat model, Life Sci. 124 (2015) 50–55. https://doi.org/10.1016/j.lfs.2014.12.020.

58 S.G. Ong, W.H. Lee, L. Theodorou, K. Kodo, S.Y. Lim, D.H. Shukla, T. Briston, S. Kiriakidis, M. Ashcroft, S.M. Davidson, P.H. Maxwell, D.M. Yellon, D.J. Hausenloy, HIF-1 reduces ischaemia-reperfusion injury in the heart by targeting the mitochondrial permeability transition pore, Cardiovasc. Res. 104 (2014) 24–36. https://doi.org/10.1093/cvr/cvu172.

59 S. Reischl, L. Li, G. Walkinshaw, L.A. Flippin, H.H. Marti, R. Kunze, Inhibition of HIF prolyl-4-hydroxylases by FG-4497 reduces brain tissue injury and edema formation during ischemic stroke, PLoS One. 9 (2014) e84767. https://doi.org/10.1371/journal.pone.0084767.

60 J. Wu, C. Bond, P. Chen, M. Chen, Y. Li, R.V. Shohet, G. Wright, HIF-1α in the heart: remodeling nucleotide metabolism, J. Mol. Cell. Cardiol. 82 (2015) 194–200. https://doi.org/10.1016/j.yjmcc.2015.01.014.

61 Y.F. Chen, S. Pandey, C.H. Day, Y.F. Chen, A.Z. Jiang, T.J. Ho, R.J. Chen, V.V. Padma, W.W. Kuo, C.Y. Huang, Synergistic effect of HIF-1α and FoxO3a trigger cardiomyocyte apoptosis under hyperglycemic ischemia condition, J. Cell. Physiol. 233 (2018) 3660–3671. https://doi.org/10.1002/jcp.26235.

62 X. Zhao, L. Liu, R. Li, X. Wei, W. Luan, P. Liu, J. Zhao, Hypoxia-Inducible Factor 1-α (HIF-1α) induces apoptosis of human uterosacral ligament fibroblasts through the death receptor and mitochondrial pathways, Med. Sci. Monit. 24 (2018) 8722–8733. https://doi.org/10.12659/MSM.913384.

63 S.C. Choi, Y.F. Ho, W.P. Tsang, T.T. Kwok, The roles of HIF-1α and p53 in severe hypoxia induced apoptosis, Cancer Res. 68 (2008) 1820.

64 H. Menrad, C. Werno, T. Schmid, E. Copanaki, T. Deller, N. Dehne, B. Brüne, Roles of hypoxia-inducible factor-1alpha (HIF-1alpha) versus HIF-2alpha in the survival of hepatocellular tumor spheroids, Hepatology 51 (2010) 2183–2192.

65 J. Yang, F. He, Q. Meng, Y. Sun, W. Wang, C. Wang. Inhibiting HIF-1α decreases expression of TNF-α and Caspase-3 in specific brain regions exposed kainic acid-induced status epilepticus, Cell. Physiol. Biochem. 38 (2016) 75–82. ttps://doi.org/10.1159/000438610.

66 Y.L. Yeh, W.S. Hu, W.J. Ting, C.Y. Shen, H.H. Hsu, L.C. Chung, C.C. Tu, S.H. Chang, C. H. Day, Y. Tsai, C.Y. Huang, Hypoxia augments increased HIF-1α and reduced survival protein p-Akt in Gelsolin (GSN)-dependent cardiomyoblast cell apoptosis, Cell. Biochem. Biophys. 74 (2016) 221–228. https://doi.org/10.1007/s12013-016-0729-6.

67 T.A. Intihar, E.A. Martinez, R. Gomez-Pastor, Mitochondrial dysfunction in Huntington's disease; interplay between HSF1, p53 and PGC-1α transcription factors, Front. Cell. Neurosci. 13 (2019) 103. https://doi.org/10.3389/fncel.2019.00103.

68 M. Nasehi, S. Torabinejad, M. Hashemi, S. Vaseghi, M.R. Zarrindast, Effect of cholestasis and NeuroAid treatment on the expression of Bax, Bcl-2, Pgc-1α and Tfam genes involved in apoptosis and mitochondrial biogenesis in the striatum of male rats, Metab. Brain Dis. 35 (2020) 183–192. https://doi.org/10.1007/s11011-019-00508-y.

69 Q. Zhang, X.C. Liang. Effects of mitochondrial dysfunction via AMPK/PGC-1α signal pathway on pathogenic mechanism of diabetic peripheral neuropathy and the protective effects of Chinese medicine, Chin. J. Integr. Med. 25 (2019) 386–394. https://doi.org/10.1007/s11655-018-2579-0.

70 K. Bremer, K.M. Kocha, T. Snider, C.D. Moyes, Sensing and responding to energetic stress: The role of the AMPK-PGC1α-NRF1 axis in control of mitochondrial biogenesis in fish, Comp. Biochem. Physiol. B Biochem. Mol. Biol. 199 (2016) 4–12. https://doi.org/10.1016/j.cbpb.2015.09.005.

71 H. Chong, Z. Wei, M. Na, G. Sun, S. Zheng, X. Zhu, Y. Xue, Q. Zhou, S. Guo, J. Xu, H. Wang, L. Cui, C.Y. Zhang, X. Jiang, D. Wang, The PGC-1α/NRF1/miR-378a axis protects vascular smooth muscle cells from FFA-induced proliferation, migration and inflammation in atherosclerosis, Atherosclerosis 297 (2002) 136–145. https://doi.org/10.1016/j.atherosclerosis.2020.02.001.

Abbreviations

DMEM, Dulbecco's modified Eagle's medium; FBS, Fetal bovine serum; HIF, Hypoxia-inducible factors; PCR, Polymerase chain reaction

Figures

Figure 1

Evaluation of cell proliferation. Cardiomyocyte proliferation was monitored using an ACEA iCell real-time cell proliferation analyzer. Cell proliferation was monitored every 10 min for 24 h. A, B. Left, the proliferation of cardiomyocytes under normoxia; right, proliferation of cardiomyocytes under hypoxia (1% O2).

Figure 2

Assessment of cardiomyocyte apoptosis under hypoxia. A. Measurement of caspase-3 activity, *P < 0.05, vs. H9C2. #P < 0.05, vs. pCDH-CMV or pGreenPuro. B. Followed by the NRF-1 overexpression (pCDH-NRF1), compared to those in pCDH-CMV, the levels of NRF-1, BCL-2, BCL-xL, and Bax changed after the cells were subjected to hypoxia (at 1% O2) for 0, 1, 2, 3, 6, 12, and 24 h. C. Following NRF-1 inhibition (sh-NRF1), the levels of NRF-1, BCL-2, BCL-xL, and Bax changed after the cells were subjected to hypoxia (at 1% O2) for 0, 1, 2, 3, 6, 12, and 24 h. Bad: BCL-associated agonist of cell death; Bak: BCL-2 homologous antagonist/killer; Bax: BCL-2-associated X protein; BCL-2: B-cell lymphoma 2; BCL-xl: BCL-extra-large; NRF-1: nuclear respiratory factor-1.

Figure 3

Effect of NRF-1 on HIF-1α expression. A. The binding level of NRF-1 to the binding element in the Hif-1α promoter region was determined using ChIP. B. Effects of NRF-1 on Hif-1α mRNA were assessed by a quantitative polymerase chain reaction. **P < 0.01, ***P < 0.01, vs. pCDH-CMV or pGreenPuro. Data are presented as mean ± standard deviation (n = 3). C. Western blotting was performed to ascertain the effect of NRF-1 on HIF-1α protein levels after the cells were subjected to hypoxia for 0, 1, 2, 3, 6, 12, and 24 h. ChIP: chromatin immunoprecipitation; HIF: hypoxia-inducible factor; NRF-1: nuclear respiratory factor-1.

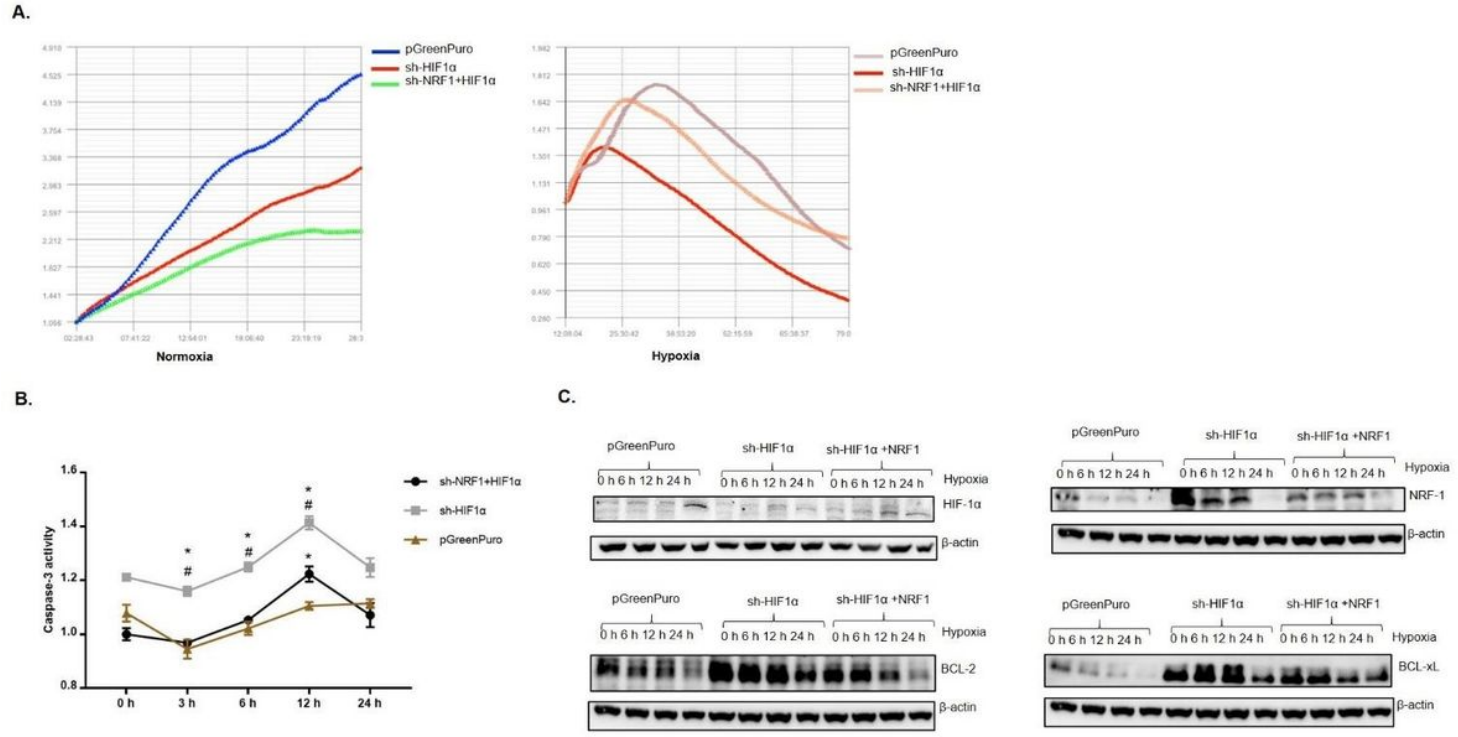

Figure 4

Effect of NRF-1 and HIF-1α on cardiomyocyte apoptosis. A. Evaluation of cardiomyocyte proliferation in each group. B. Caspase-3 activity under hypoxia. C. The levels of HIF-1α, NRF-1, BCL-2, and BCL-xL were determined by western blotting. *P < 0.05 vs. pGreenPuro. #P < 0.05 showed sh-HIF1α vs. sh-HIF1α+NRF1. BCL-2: B-cell lymphoma 2; BCL-xl: BCL-extra-large; HIF: hypoxia-inducible factor; NRF-1: nuclear respiratory factor-1.

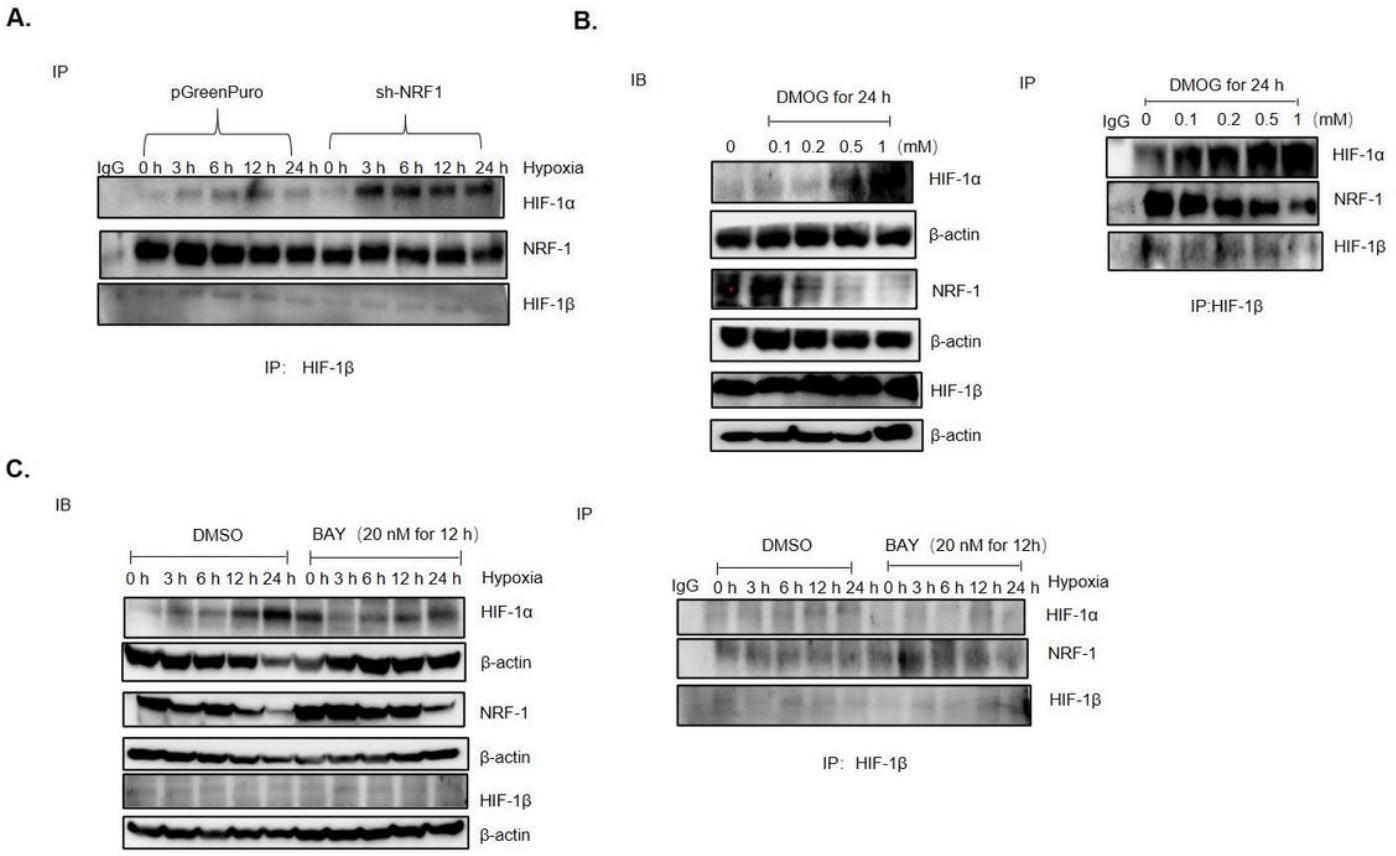

Figure 5

Immunoprecipitation for determination of the level of NRF-1, HIF-1α, and HIF-1β binding. A. The binding levels of NRF-1, HIF-1α, and HIF-1β were studied after the inhibition of NRF-1 (sh-NRF1) under hypoxia. B. After treatment with different DMOG concentrations (0, 0.1, 0.2, 0.5, and 1 mM), the expression and binding levels of NRF-1, HIF-1α, and HIF-1β in cardiomyocytes were observed. C. After treatment with 20 nM BAY 87-2243 for 12 h, the expression and binding levels of NRF-1, HIF-1α, and HIF-1β were observed under hypoxia for different durations. DMOG: dimethyloxallyl glycine; HIF: hypoxia-inducible factor; NRF-1: nuclear respiratory factor-1.

Figure 6

Role of PGC-1α in the competitive binding of HIF-1α and NRF-1 with HIF-1β. A. Left, levels of PGC-1α in each group; right, binding levels of PGC-1α and NRF-1 under hypoxia. B. Left, the effect of different concentrations of DMOG on PGC-1α; right, binding levels of HIF-1α, NRF-1, and PGC-1α with HIF-1β. C. Left, changes in the levels of HIF-1α, NRF-1, PGC-1α, and HIF-1β after treatment with ZLN005 for 24 h under hypoxia for 0, 6, 12, and 24 h; right, binding levels of HIF-1α, NRF-1, and PGC-1α with HIF-1β. DMOG: dimethyloxallyl glycine; HIF: hypoxia-inducible factor; NRF-1: nuclear respiratory factor-1; PGC-1α: peroxisome proliferator-activated receptor gamma coactivator 1-alpha.

Supplementary Files

This is a list of supplementary files associated with this preprint. Click to download.

- SupplementaryFigure.pdf
- Video58.rar
- Video14.rar